Journal of Computational and Applied Mathematics 410 (2022) 114013

Contents lists available at ScienceDirect

Journal of Computational and Applied Mathematics

journal homepage: www.elsevier.com/locate/cam

A lowest-order free-stabilization Virtual Element Method for the Laplacian eigenvalue problem

Jian Meng [a], Xue Wang [b], Linlin Bu [a], Liquan Mei [a,*]

[a] School of Mathematics and Statistics, Xi'an Jiaotong University, Xi'an, Shaanxi, 710049, PR China
[b] School of Big Date and Cloud Computation, Xi'an Vocational University of Information, Shenhe Road, 710125, Xi'an, Shaanxi, PR China

ARTICLE INFO

Article history:
Received 17 August 2021
Received in revised form 9 December 2021

MSC:
65N25
65N30
65N15

Keywords:
Free-stabilization VEM
Polygonal mesh
Eigenvalue problem
A priori error estimate

ABSTRACT

In this paper, we propose a Virtual Element Method (VEM) for the Laplacian eigenvalue problem, which is designed to avoid the requirement of the stabilization terms in standard VEM bilinear forms. In the present method, the constructions of the bilinear forms depend on higher order polynomial projection. To exactly compute the bilinear forms, we need to modify the virtual element space associated to the higher order polynomial projection. Meanwhile, the continuity and coercivity of the discrete VEM bilinear forms depend on the number of vertices of the polygon. By the spectral approximation theory of compact operator and the projection and interpolation error estimates, we prove correct spectral approximation and error estimates for the VEM discrete scheme. Finally, we show numerical examples to verify the theoretical results, including the Laplace eigenvalue problem and the Steklov eigenvalue problem.

1. Introduction

In modern scientific and engineering applications, the eigenvalue problems arising from partial differential equations(PDEs) are of fundamental importance in many fields [1–4]. There are many numerical methods to solve the Laplace eigenvalue problem [5–8] and finite element method (FEM) is an effective numerical method for the eigenvalue problem [9–13]. The virtual element method (VEM), introduced in [14], is a successful extension of FEM to polygonal/polyhedral meshes. The virtual element space contains a polynomial subspace and the remaining non-polynomial virtual subspace through the introduction of suitable projection operators allowed to be computed by using the degrees of freedom (DoFs) related to the virtual element space. The basis functions are defined by the local PDE problem and never need the explicit expression. The VEM is also attractive apart from the mere possibility to use polytopal meshes and is promising in problems related to high-order PDEs and in problems where several useful features are requested at the same time. We mention the recent works [15,16] for a thorough description of the state of the art. To date, the VEM has been successfully applied to different fields. Regarding the VEMs for eigenvalue problems, there have been the Steklov eigenvalue problem [17–19], the Laplacian eigenvalue problem [20–24], the acoustic vibration problem [25], the vibration and buckling problems of Kirchhoff plate [26–28], the linear elasticity eigenvalue problem [29], the transmission eigenvalue problem [30,31], the Stokes eigenvalue problem [32] and the recent review paper [33].

* Corresponding author.
E-mail addresses: mengjian0710@163.com (J. Meng), xuewang1031@163.com (X. Wang), bulinlinlin@126.com (L. Bu), lqmei@mail.xjtu.edu.cn (L. Mei).

https://doi.org/10.1016/j.cam.2021.114013
0377-0427/

In the standard VEM scheme, a bilinear form includes consistency and stabilization parts, where the consistency on polynomial spaces is assured by the consistency term and the stability of VEM scheme is guaranteed by the other. As discussed in [34], the stabilization terms on both sides of the VEMs of the eigenvalue problems might have dramatic effects on the performance of the VEM. They also presented the behavior of the Laplace eigenvalues for the VEM without stabilization terms on both sides. The numerical results are not stable because of the lack of the stabilization term. It is nontrivial to develop the free-stabilization VEM for the eigenvalue problems. Recently, Berrone, Borio and Marcon [35] introduced an Enlarged Enhancement VEM to delete the stabilization term in the VEM bilinear form by using the higher order polynomial projection and generalizing the virtual element space to allow the computation of such projection. Under suitable condition, they have proved the well-posedness and error estimates of the Poisson equation, which constitutes a stepping stone for more challenging problems. Moreover, it is clear that the free-stabilization VEM is also meaningful for *a posteriori* error estimate of the VEM, because it can remove some theoretical derivations caused by the stabilization terms of the VEMs [19,29].

The aim of this paper is to extend the work in [35] to construct the free-stabilization VEM for the eigenvalue problem, which can ignore the effects of the stabilization term on both sides of the VEM of the eigenvalue problem. In this paper, we shall present the *a priori* error estimates for the free-stabilization VEM approximation for the self-adjoint Laplacian-type eigenvalue problem. Note that there is not k-consistency and stability properties as proved in the standard VEM scheme [18,21]. We prove the correct spectral approximation of the VEM for the eigenvalue problem and establish the optimal *a priori* error estimates for the discrete eigenvalues and eigenfunctions of the VEM scheme. Numerical results are shown to support the theoretical analysis. According to existing theory [35], we only focus on the simplest free-stabilization approximation on the 2D case. The higher order and dimensional free-stabilization VEMs for the eigenvalue problems are under our investigation.

Throughout the paper, we will use the standard notation for Sobolev space $W^{s,p}(D)$ equipped with the norm $\|\cdot\|_{s,p,D}$ and seminorm $|\cdot|_{s,p,D}$ in a bounded domain D. For $p = 2$, we denote $H^s(D) = W^{s,2}(D)$, and the subscript p in the associated norm and seminorm will be omitted. The space $H^0(D)$ coincides with $L^2(D)$, and the inner product on $L^2(D)$ is denoted by $(\cdot,\cdot)_D$. The subscript D will be omitted when D denotes the whole computational domain. For a nonnegative integer k, $\mathbb{P}_k(D)$ denotes the space of polynomials on D of degree at most k. As usual, we use bold fonts to express vector and matrix variables, operators and spaces. Let C be a constant independent of the mesh size.

This paper is organized as follows: In this section, we introduce the motivation for this work. In Section 2, we introduce the Laplace eigenvalue problem and the relevant continuous solution operator. In Section 3, we present the free-stabilization virtual element approximation and derive the error estimates for the source problem. In Section 4, we prove the spectral approximation and the optimal *a priori* error estimates of the eigenvalue problem. In Section 5, we demonstrate numerical experiments to validate the theoretical results. Finally, conclusions are drawn in Section 6.

2. The eigenvalue problem and its corresponding source problem

Let $\Omega \subseteq \mathbb{R}^2$ be a bounded domain with the Lipschitz boundary $\partial\Omega$. The Laplace eigenvalue problem is stated as follows: find $u \neq 0$ and $\lambda \in \mathbb{R}$ such that

$$\Delta u = \lambda u \text{ in } \Omega, \quad \text{and} \quad u = 0 \text{ on } \partial\Omega. \tag{2.1}$$

The corresponding variational formulation is to find nonzero $(\lambda, u) \in \mathbb{R} \times H_0^1(\Omega)$ such that

$$a(u, v) = \lambda(u, v), \ \ \forall v \in H_0^1(\Omega), \tag{2.2}$$

where we denote $a(u, v) := (\nabla u, \nabla v)$. In order to estimate the error of the approximate solution, we consider the corresponding source problem of (2.2): for any given $f \in H_0^1(\Omega)$, find $\mu \in H_0^1(\Omega)$ such that

$$a(\mu, v) = (f, v), \ \ \forall v \in H_0^1(\Omega). \tag{2.3}$$

The well-posedness of (2.3) follows from the Poincaré inequality and the Lax–Milgram Theorem. By the Riesz representation theorem, we can introduce the solution operator $T : H_0^1(\Omega) \to H_0^1(\Omega)$ defined by $Tf = \mu$ with $\mu \in H_0^1(\Omega)$ being the solution of (2.3). Since the eigenvalue problem (2.2) does not admit the null eigenvalue, then λ is an eigenvalue of (2.2) if and only if $1/\lambda$ is an eigenvalue of T associated to the same eigenvector $T(\lambda u)$.

According to the regularity for the solution to the Laplace problem, we assume that for a datum $f \in L^2(\Omega)$, the solution μ of the source problem (2.3) has the regularity $\mu \in H^{1+r}(\Omega)$ with $r > 1/2$ depending on the domain Ω. Furthermore, the solution μ satisfies $\|\mu\|_{1+r} \leq C\|f\|_0$. It has been proved that $r \geq 1$ if the domain is convex and $r \geq \pi/\omega - \varepsilon$ for any $\varepsilon > 0$ with the maximum interior angle ω of Ω. Then we easily check from the symmetry of the bilinear forms $a(\cdot,\cdot)$ and $(\cdot,\cdot)$, the regularity and the compact inclusion $H^{1+r}(\Omega) \hookrightarrow H_0^1(\Omega)$ that T is a symmetric and compact linear operator [10,11].

3. Free-stabilization VEM

Let $\mathcal{T}_h$ be a non-overlapping partition of Ω with N^E elements. For each element $E \in \mathcal{T}_h$ with N_E^V vertices, we denote its boundary by ∂E, its unit outer normal by $\boldsymbol{\nu}_E$, its diameter by h_E and the ith vertex by V_i, respectively. The mesh size is denoted as $h := \max\{h_E : E \in \mathcal{T}_h\}$. The mesh regularity assumptions are shown as follows [14,36]: there exists a positive constant C independent of mesh size such that

(i) every polygonal element E is star-shaped with respect to a disk with the radius $\geq Ch_E$;
(ii) every edge $e \in \partial E$ with the length h_e satisfies $h_e \geq Ch_E$.

We denote by $(\cdot,\cdot)_E$ and $a^E(\cdot,\cdot)$ the restriction to the element E of the corresponding bilinear forms. We first introduce a projection operator $\Pi_{1,E}^{\nabla} : H^1(E) \to \mathbb{P}_1(E)$ by

$$a^E(\Pi_{1,E}^{\nabla} v - v, p_1) = 0, \quad \forall v \in H^1(E),\ p_1 \in \mathbb{P}_1(E) \tag{3.1}$$

$$\frac{1}{N_E^V}\sum_{i=1}^{N_E^V}(\Pi_{1,E}^{\nabla} v - v)(V_i) = 0. \tag{3.2}$$

Inspired by Ref. [35], we present the construction of the local enlarged enhancement virtual element space of order 1 based on the use of higher order polynomial projection for given $l \in \mathbb{N}$,

$$\mathcal{V}_{1,l}(E) = \Big\{ v \in H^1(E),\, v|_{\partial E} \in C^0(\partial E) : v|_e \in \mathbb{P}_1(e), \forall e \in \partial E,\ \Delta v \in \mathbb{P}_{l+1}(E), \\ (\Pi_{1,E}^{\nabla} v - v, p_{l+1})_E = 0,\ \forall p_{l+1} \in \mathbb{P}_{l+1}(E) \Big\}.$$

For each $v \in \mathcal{V}_{1,l}(E)$, we can still choose the values at N_E^V vertices in E as the unisolvent degrees of freedom (DoFs) of the space $\mathcal{V}_{1,l}(E)$ [14,35]. Moreover, due to the elaborate discussion in [35], the given number l must satisfy the following condition for the lowest case,

$$(l+1)(l+2) \geq N_E^V - 1, \tag{3.3}$$

which is used to prove the well-posedness of the corresponding discrete source problem. We list the given number l related to every element E (denoted by $\boldsymbol{\ell}(E)$) into a vector and denote the vector by $\boldsymbol{\ell} \in \mathbb{N}^{N^E}$. Then we construct the global virtual element space as follows:

$$\mathcal{V}_{1,\boldsymbol{\ell}}^0 = \{v \in H_0^1(\Omega) : v|_E \in \mathcal{V}_{1,l}(E),\ \forall E \in \mathcal{T}_h\}.$$

We recall the projection error and interpolation error under the assumptions of the mesh decomposition.

Proposition 3.1 ([18,35,37]). *For $v \in H^{1+s}(E)$ with $0 \leq s \leq 1$, there exists $v_\pi \in \mathbb{P}_1(E)$ such that*

$$\|v - v_\pi\|_{0,E} + h_E|v - v_\pi|_{1,E} \leq Ch_E^{1+s}\|v\|_{1+s,E}. \tag{3.4}$$

Proposition 3.2 ([18,35,38]). *For $v \in H^{1+s}(E)$ with $0 \leq s \leq 1$, there exists $v_I \in \mathcal{V}_{1,l}(E)$ such that*

$$\|v - v_I\|_{0,E} + h_E|v - v_I|_{1,E} \leq Ch_E^{1+s}\|v\|_{1+s,E}. \tag{3.5}$$

Next, we give the virtual element scheme without stabilization terms for the eigenvalue problem. Let $\Pi_{1,E}^0$ be the standard scalar $L^2(E)$ projection from $\mathcal{V}_{1,l}(E)$ to $\mathbb{P}_1(E)$ and $\boldsymbol{\Pi}_{l,E}^0\nabla$ be the $L^2(E)$ projection of the gradient of functions in $\mathcal{V}_{1,l}(E)$ to $[\mathbb{P}_l(E)]^2$, that is, they can be explicitly expressed as

$$(\Pi_{1,E}^0 v - v, p_1)_E = 0, \qquad \forall v \in \mathcal{V}_{1,l}(E),\ p_1 \in \mathbb{P}_1(E), \tag{3.6}$$

$$(\boldsymbol{\Pi}_{l,E}^0\nabla v - \nabla v, \boldsymbol{p}_l)_E = 0, \qquad \forall v \in \mathcal{V}_{1,l}(E),\ \boldsymbol{p}_l \in [\mathbb{P}_l(E)]^2. \tag{3.7}$$

Note that, integrating by parts for (3.7), we have

$$(\boldsymbol{\Pi}_{l,E}^0\nabla v, \boldsymbol{p}_l)_E = (\nabla v, \boldsymbol{p}_l)_E = \int_{\partial E} v\boldsymbol{p}_l \cdot \boldsymbol{\nu}_E \mathrm{d}s - \int_E \mathrm{div}(\boldsymbol{p}_l) v \mathrm{d}x. \tag{3.8}$$

Since $v|_e \in \mathbb{P}_1(e),\ \forall e \in \partial E$, then the first term in (3.8) can be computed on each edge of E. Moreover, it follows from the definition of $\mathcal{V}_{1,l}(E)$ that $\int_E \mathrm{div}(\boldsymbol{p}_l) v \mathrm{d}x = \int_E \mathrm{div}(\boldsymbol{p}_l)\Pi_{1,E}^{\nabla} v \mathrm{d}x$, then the second term in (3.8) is computable from the computation of the projection operator $\Pi_{1,E}^{\nabla}$. We can also check from the definition of $\mathcal{V}_{1,l}(E)$ and (3.6) that $\Pi_{1,E}^0 = \Pi_{1,E}^{\nabla}$ in the lowest case.

The free-stabilization virtual element scheme is to find $(\lambda_h, u_h) \in \mathbb{R} \times \mathcal{V}_{1,\boldsymbol{\ell}}^0$ such that

$$a_h(u_h, v_h) = \lambda_h b_h(u_h, v_h), \quad \forall v_h \in \mathcal{V}_{1,\boldsymbol{\ell}}^0, \tag{3.9}$$

where

$$a_h(u_h, v_h) = \sum_{E\in\mathcal{T}_h} a_h^E(u_h, v_h) \quad \text{with} \quad a_h^E(u_h, v_h) = (\boldsymbol{\Pi}_{l,E}^0 \nabla u_h, \boldsymbol{\Pi}_{l,E}^0 \nabla v_h)_E,$$
$$b_h(u_h, v_h) = \sum_{E\in\mathcal{T}_h} b_h^E(u_h, v_h) \quad \text{with} \quad b_h^E(u_h, v_h) = (\Pi_{1,E}^0 u_h, \Pi_{1,E}^0 v_h)_E.$$

As the continuous case, we can introduce the discrete solution operator $T_h : H_0^1(\Omega) \to \mathcal{V}_{1,\ell}^0 \subseteq H_0^1(\Omega)$ defined by $T_h f = \mu_h$, where μ_h is the solution to the corresponding discrete source problem: for any given $f \in H_0^1(\Omega)$, find $\mu_h \in \mathcal{V}_{1,\ell}^0$ such that

$$a_h(\mu_h, v_h) = b_h(f, v_h), \quad \forall v_h \in \mathcal{V}_{1,\ell}^0. \tag{3.10}$$

The continuity and coercivity of $a_h(\cdot,\cdot)$ have been proved in [35, Theorem 2]. Then we have the existence and uniqueness of a discrete solution to the problem (3.10). Thus the discrete solution operator T_h is well-defined. Moreover, λ_h is an eigenvalue of problem (3.9) if and only if $1/\lambda_h$ is an eigenvalue of T_h, with the same multiplicity and corresponding eigenfunction u_h. The error bound has also been proved in [35, Theorem 3] as follows:

$$\|\mu - \mu_h\|_1 \le C \sum_{E\in\mathcal{T}_h} \left(\|\mu - \mu_I\|_{1,E} + \|\boldsymbol{\Pi}_{l,E}^0 \nabla\mu - \nabla\mu\|_{0,E} + \|f - \Pi_{1,E}^0 f\|_{0,E}\right).$$

From the projection and interpolation error estimates in Propositions 3.1 and 3.2, and the regularity result, the error estimate becomes

$$\begin{aligned} \|\mu - \mu_h\|_1 &\le C \sum_{E\in\mathcal{T}_h} \left(\|\mu - \mu_I\|_{1,E} + \|\boldsymbol{\Pi}_{l,E}^0 \nabla\mu - \nabla\mu\|_{0,E} + \|f - \Pi_{1,E}^0 f\|_{0,E}\right) \\ &\le C\left(h^r \|\mu\|_{1+r} + h\|f\|_1\right) \le C h^{\min\{r,1\}} \|f\|_1. \end{aligned} \tag{3.11}$$

4. Spectral approximation and a priori error estimates

Due to the spectral approximation theory of compact operator in [10], it is enough to prove the convergence of T_h to the solution operator T in the operator norm $\|\cdot\|_{\mathcal{L}(H_0^1(\Omega))}$ to derive the spectral approximation.

Theorem 4.1. *There exists a constant $C > 0$ such that*

$$\|T - T_h\|_{\mathcal{L}(H_0^1(\Omega))} \le C h^{\min\{r,1\}}. \tag{4.1}$$

Proof. By the definitions of the operator norm $\|\cdot\|_{\mathcal{L}(H_0^1(\Omega))}$ and the solution operators, and the error estimate in (3.11) we have

$$\|T - T_h\|_{\mathcal{L}(H_0^1(\Omega))} = \sup_{f\in H_0^1(\Omega)} \frac{\|(T - T_h)f\|_1}{\|f\|_1} = \sup_{f\in H_0^1(\Omega)} \frac{\|\mu - \mu_h\|_1}{\|f\|_1} \le C h^{\min\{r,1\}}.$$

Thus we complete the proof. □

Let λ be an eigenvalue of (2.2) with multiplicity m, and denote the corresponding eigenspace by $\mathcal{E}_\lambda$. Since $T_h \to T$ as h tends to zero, then there are m discrete eigenvalues $\lambda_h^1, \ldots, \lambda_h^m$, which are repeated according to their respective multiplicities and converge to λ[10, Section 8]. We denote $\mathcal{E}_{\lambda_h}$ be the direct sum of the eigenspaces related to the eigenvalues $\lambda_h^1, \ldots, \lambda_h^m$. The gap $\hat{\delta}$ between two subspaces X and Y of $H_0^1(\Omega)$ is defined by $\hat{\delta}(X, Y) = \max\{\delta(X, Y), \delta(Y, X)\}$, where $\delta(X, Y) = \sup_{x\in X, \|x\|_1=1} \left(\inf_{y\in Y} \|x - y\|_1\right)$, analogously for $\delta(Y, X)$. Thanks to Theorems 7.1 and 7.3 in [10], we obtain the following spectral approximation.

Theorem 4.2. *Let λ be an eigenvalue of (2.2) associated to the eigenfunction u, then there exists an eigenvalue λ_h of (3.9) associated to the eigenfunction u_h such that*

$$\hat{\delta}((\mathcal{E}_\lambda), (\mathcal{E}_{\lambda_h})) \le C h^{\min\{r,1\}}, \tag{4.2}$$
$$|\lambda - \lambda_h^i| \le C h^{\min\{r,1\}}, \quad i = 1, \ldots, m. \tag{4.3}$$

Proof. We consider $f := \lambda u \in \mathcal{E}_\lambda \subseteq H^{1+r}(\Omega)$, then it follows from the steps in Theorem 4.1 that the following error estimate of the eigenfunction holds

$$\|u - u_h\|_1 \le C h^{\min\{r,1\}} \|u\|_{1+r}, \tag{4.4}$$

which implies that

$$\|(T - T_h)|_{\mathcal{E}_\lambda}\|_{\mathcal{L}(H_0^1(\Omega))} \le Ch^{\min\{r,1\}}. \tag{4.5}$$

From Theorems 7.1 and 7.3 in [10], we have

$$\hat{\delta}((\mathcal{E}_\lambda), (\mathcal{E}_{\lambda_h})) \le C\|(T - T_h)|_{\mathcal{E}_\lambda}\|_{\mathcal{L}(H_0^1(\Omega))}, \tag{4.6}$$

$$|\lambda - \lambda_h^i| \le C\|(T - T_h)|_{\mathcal{E}_\lambda}\|_{\mathcal{L}(H_0^1(\Omega))}. \tag{4.7}$$

Substituting (4.5) into (4.6) and (4.7), we obtain (4.2) and (4.3). □

However, the order $O(h)$ is not optimal for the eigenvalue problem as the corresponding eigenfunction is smooth enough. It remains to give the optimal convergence order for the approximation of eigenvalues.

Theorem 4.3. *There exists a constant $C > 0$ such that*

$$|\lambda - \lambda_h^i| \le Ch^{2\min\{r,1\}}, \quad i = 1, \ldots, m. \tag{4.8}$$

Proof. From (2.2) and (3.9), we have

$$\begin{aligned} &a(u - u_h, u - u_h) - \lambda(u - u_h, u - u_h) = a(u_h, u_h) - \lambda(u_h, u_h) \\ &= a(u_h, u_h) - a_h(u_h, u_h) + \lambda_h^i(b_h(u_h, u_h) - (u_h, u_h)) + (\lambda_h^i - \lambda)(u_h, u_h), \end{aligned} \tag{4.9}$$

which implies that

$$\begin{aligned} (\lambda_h^i - \lambda)(u_h, u_h) = &\underbrace{a(u - u_h, u - u_h) - \lambda(u - u_h, u - u_h)}_{D_1} \\ &+ \underbrace{a_h(u_h, u_h) - a(u_h, u_h) + \lambda_h^i((u_h, u_h) - b_h(u_h, u_h))}_{D_2}. \end{aligned} \tag{4.10}$$

For the first term D_1 on the right-hand side, it follows by the Cauchy–Schwarz inequality and (4.4) that

$$D_1 \le C\|u - u_h\|_1^2 \le Ch^{2\min\{r,1\}}. \tag{4.11}$$

For the second term D_2, we have

$$\begin{aligned} D_2 &= \sum_{E\in\mathcal{T}_h} \left[(\boldsymbol{\Pi}_{l,E}^0 \nabla u_h, \boldsymbol{\Pi}_{l,E}^0 \nabla u_h)_E - (\nabla u_h, \nabla u_h)_E + \lambda_h^i((u_h, u_h)_E - (\Pi_{1,E}^0 u_h, \Pi_{1,E}^0 v_h)_E)\right] \\ &= \sum_{E\in\mathcal{T}_h} \left[(\nabla u_h - \boldsymbol{\Pi}_{l,E}^0 \nabla u_h, \boldsymbol{\Pi}_{l,E}^0 \nabla u_h - \nabla u_h)_E + \lambda_h^i(u_h - \Pi_{1,E}^0 u_h, u_h - \Pi_{1,E}^0 u_h)_E\right] \\ &\le C(\|\nabla u_h - \boldsymbol{\Pi}_{l,E}^0 \nabla u_h\|_0^2 + \|u_h - \Pi_{1,E}^0 u_h\|_0^2) \\ &\le Ch^{2\min\{r,1\}}, \end{aligned}$$

where we have used the definitions of $\boldsymbol{\Pi}_{l,E}^0 \nabla$ and $\Pi_{1,E}^0$, the Cauchy–Schwarz inequality and Proposition 3.1.

On the left-hand side, from the facts $b_h(u_h, u_h) \to (u_h, u_h)$ and $\lambda_h^i \to \lambda$ as $h \to 0$, (3.9) and the coercivity of $a_h(\cdot, \cdot)$, we obtain

$$b_h(u_h, u_h) = \frac{a_h(u_h, u_h)}{\lambda_h^i} \ge C\frac{\|u_h\|_1^2}{\lambda_h^i} := \hat{C} > 0. \tag{4.12}$$

Collecting the above estimates, we complete the proof. □

Next, we also improve the error bound for the eigenfunction u with respect to the L^2-norm by the Aubin–Nitsche technique. Let (λ, u) and (λ_h, u_h) be the eigenpairs of (2.2) and (3.9), respectively. We consider the following dual problem: find $p \in H_0^1(\Omega)$ such that

$$a(\varphi, p) = (\varphi, u - u_h), \quad \forall \varphi \in H_0^1(\Omega). \tag{4.13}$$

Then we have by the regularity assumption,

$$\|p\|_{1+r} \le C\|u - u_h\|_0. \tag{4.14}$$

Theorem 4.4. *There exists a constant $C > 0$ such that*

$$\|u - u_h\|_0 \le Ch^{2\min\{r,1\}}. \tag{4.15}$$

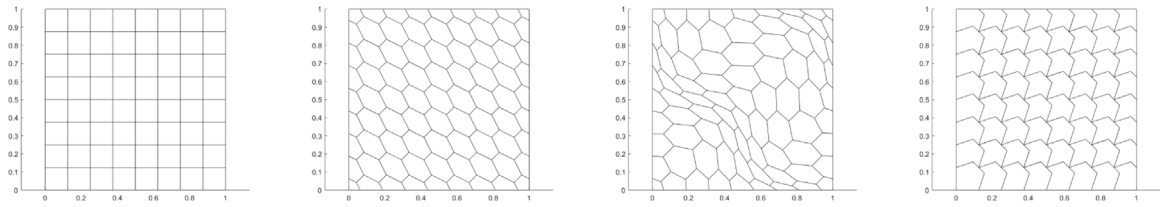

(a) $\mathcal{T}_h^1$ (b) $\mathcal{T}_h^2$ (c) $\mathcal{T}_h^3$ (d) $\mathcal{T}_h^4$

Fig. 1. Test 5.1: basic sample meshes on the square domain Ω_S.

Proof. Let $\varphi = u - u_h$ in (4.13), then it follows from (2.2), (3.9), the definitions of $\boldsymbol{\Pi}_{l,E}^0\nabla$ and $\Pi_{1,E}^0$, the Cauchy–Schwarz inequality, (4.4), (4.8) and (4.14) that

$$
\begin{aligned}
&\|u-u_h\|_0^2 = a(u-u_h,p)\\
&= a(u-u_h,p-p_I)+a(u-u_h,p_I)\\
&= a(u-u_h,p-p_I)+a_h(u_h,p_I)-a(u_h,p_I)+\lambda(u,p_I)-\lambda_h b_h(u_h,p_I)\\
&\le C\Bigg(a(u-u_h,p-p_I)+\sum_{E\in\mathcal{T}_h}\big((\boldsymbol{\Pi}_{l,E}^0\nabla u_h,\boldsymbol{\Pi}_{l,E}^0\nabla p_I)_E-(\nabla u_h,\nabla p_I)_E+(\lambda-\lambda_h)(u,p_I)_E\\
&\quad+\lambda_h((u,p_I)_E-(\Pi_{1,E}^0u_h,\Pi_{1,E}^0p_I)_E)\big)\Bigg)\\
&\le C\Bigg(a(u-u_h,p-p_I)+\sum_{E\in\mathcal{T}_h}\big((\nabla u_h-\boldsymbol{\Pi}_{l,E}^0\nabla u_h,\boldsymbol{\Pi}_{l,E}^0\nabla p_I-\nabla p_I)_E+(\lambda-\lambda_h)(u,p_I)_E\\
&\quad+\lambda_h(u-\Pi_{1,E}^0u+\Pi_{1,E}^0u-\Pi_{1,E}^0u_h+\Pi_{1,E}^0u_h-u_h,p_I-\Pi_{1,E}^0p_I)_E\\
&\quad+(u_h-\Pi_{1,E}^0u_h,p_I-\Pi_{1,E}^0p_I)_E\big)\Bigg)\\
&\le Ch^r\sum_{E\in\mathcal{T}_h}\big(\|u-u_h\|_{1,E}+\|\nabla u_h-\boldsymbol{\Pi}_{l,E}^0\nabla u_h\|_{0,E}+\|u_h-\Pi_{1,E}^0u_h\|_{0,E}\big)\|u-u_h\|_0,
\end{aligned}
$$

which implies that (4.15) holds by (4.4) and Proposition 3.1. □

5. Numerical results

5.1. The Laplace eigenvalue problem

To complete the free-stabilization VEM, we need to fix the parameter l. We are interested in the influence of the given parameter l. Without loss of generality, we here discuss the performance behavior of the free-stabilization VEM when taking different parameters $l = 0, 1$, respectively. By the sufficient condition (3.3), the method is only valid for the triangular mesh if $l = 0$ and is effective on the polygons up to 7 edges for the choice $l = 1$. To observe the above behavior, we first consider the eigenvalue problem (2.1) on the unit square domain $\Omega_S = [0, 1]^2$. Then its analytic solutions are known and the first four eigenvalues and corresponding eigenfunctions are

$$
\begin{aligned}
&\lambda_1 = 2\pi^2 \approx 19.73920880218, && u_1(x,y) = \sin\pi x\sin\pi y,\\
&\lambda_2 = 5\pi^2 \approx 49.34802200545, && u_2(x,y) = \sin 2\pi x\sin\pi y,\\
&\lambda_3 = 5\pi^2 \approx 49.34802200545, && u_3(x,y) = \sin\pi x\sin 2\pi y,\\
&\lambda_4 = 8\pi^2 \approx 78.95683520872, && u_4(x,y) = \sin 2\pi x\sin 2\pi y.
\end{aligned}
$$

According to the regularity of the eigenfunctions, we know from Theorem 4.3 that the theoretical convergence rate of the approximate eigenvalue is $O(h^2)$, equivalently with $O(N^{-1})$ as the number N of the DoFs increases. For this domain, we use the following four mesh decompositions: square mesh $\mathcal{T}_h^1$, conforming and nonconforming hexagonal meshes $\mathcal{T}_h^2$ and $\mathcal{T}_h^3$, non-convex mesh $\mathcal{T}_h^4$, as shown in Fig. 1.

We compute the first four eigenvalues by using the free-stabilization VEM with $l = 0, 1$ in Tables 1 and 2. To observe the convergence rate, we compute error quantity $\varepsilon_{\lambda,i} = |\lambda_{h,i} - \lambda_i|$ $(i = 1, 2, 3, 4)$ and plot them in Figs. 2 and 3.

From Table 1 and Fig. 2, the free-stabilization VEM scheme with $l = 0$ leads to wrong eigenvalues and wrong convergence rates for the adopted polygonal meshes. Especially, the free-stabilization VEM does not work when we use

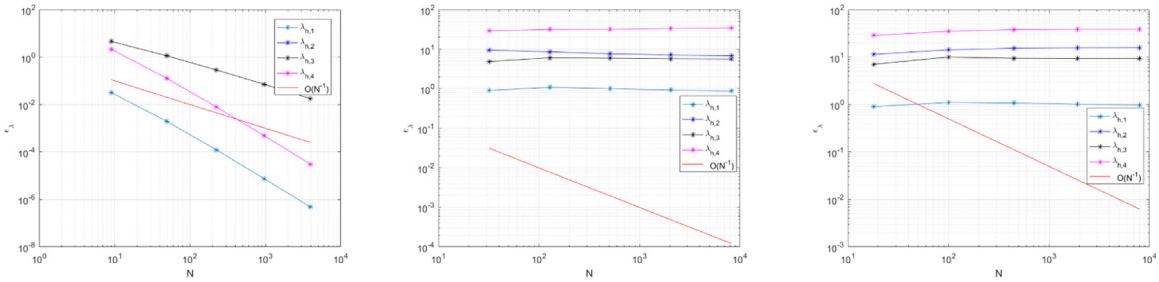

(a) $\mathcal{T}_h^1$ (b) $\mathcal{T}_h^2$ (c) $\mathcal{T}_h^3$

Fig. 2. Test 5.1: the error of the first four Laplace eigenvalues with $l = 0$ on Ω_S.

Table 1
Test 5.1: the first four Laplace eigenvalues computed by the free-stabilization VEM with $l = 0$ on Ω_S.

Mesh	N	$\lambda_{h,1}$	$\lambda_{h,2}$	$\lambda_{h,3}$	$\lambda_{h,4}$
$\mathcal{T}_h^1$	9	19.70718269985	53.92258478405	53.92258478405	76.80000000000
	49	19.73724101258	50.49758222718	50.49758222718	78.82873079938
	225	19.73908636870	49.63398622760	49.63398622760	78.94896405032
	961	19.73920115882	49.41940436973	49.41940436973	78.95634547482
	3969	19.73920832461	49.36586052434	49.36586052434	78.95680463529
$\mathcal{T}_h^2$	32	18.83507318653	39.83787141388	44.46209341594	49.94916999900
	128	18.64579342393	40.74149394332	43.27772096206	47.51659701237
	512	18.73044437378	41.65792138145	43.42510463202	47.06961246963
	2048	18.81372336966	42.20387993120	43.60436237792	45.52037048881
	8192	18.86516779247	42.49608513433	43.72619355276	44.88154853964
$\mathcal{T}_h^3$	32	18.83760719495	37.86678957185	42.28293260858	50.32212495730
	128	18.62682173350	35.06329873513	39.28371813300	43.83335223626
	512	18.65816655674	33.93552506091	39.90638620114	41.16287009213
	2048	18.71935574031	33.56761400233	39.99426601967	40.48334764074
	8192	18.76246355473	33.47101954427	40.01932081873	40.28080924301
$\mathcal{T}_h^4$	–	–	–	–	–

Table 2
Test 5.1: the first four Laplace eigenvalues computed by the free-stabilization VEM with $l = 1$ on Ω_S.

Mesh	N	$\lambda_{h,1}$	$\lambda_{h,2}$	$\lambda_{h,3}$	$\lambda_{h,4}$
$\mathcal{T}_h^1$	9	29.85083669673	101.30326305648	101.30326305648	256.00000000000
	49	22.08001973769	60.23907620321	60.23907620321	119.40334678695
	225	20.31352673853	51.95403586241	51.95403586241	88.32007895077
	961	19.88211972809	49.99245834721	49.99245834721	81.25410695410
	3969	19.77489492900	49.50869296585	49.50869296585	79.52847891236
$\mathcal{T}_h^2$	32	22.16914208328	58.85442579448	66.84270965360	109.21270353508
	128	20.47074375385	52.13243488883	54.23342332930	89.23187504877
	512	19.93874083196	50.10749033587	50.63210220786	81.94277915020
	2048	19.79123463436	49.54670012497	49.67716022997	79.74859129310
	8192	19.75248809402	49.39883517731	49.43137127052	79.15982000864
$\mathcal{T}_h^3$	32	22.54848463685	59.78379488587	69.36068499186	111.91544830011
	128	20.69346040813	53.16497726861	55.06171259494	88.65504080973
	512	20.02457236791	50.49818125273	50.93435168390	81.66294153214
	2048	19.81694723946	49.66159580497	49.76632673068	79.67724510530
	8192	19.75943396226	49.42936425034	49.45514353306	79.14296318220
$\mathcal{T}_h^4$	33	21.47110123969	53.83482693134	56.96056711337	87.16720832377
	161	20.24042899970	50.94414319257	51.71196307865	84.20036213150
	705	19.86944150683	49.77965594184	49.97694331277	80.60069585396
	2945	19.77355991588	49.46118264859	49.51088822915	79.39347893268
	12033	19.74881780944	49.37887199672	49.39130470338	79.07068827621

the non-convex mesh $\mathcal{T}_h^4$. By increasing the value of l, we observe from Table 2 that our results are very close to the exact eigenvalues as the number of the DoFs increases. Moreover, the second order convergence is observed from Fig. 3 for all the used meshes, which demonstrates the theoretical result in Theorem 4.3 and the optimality of the numerical

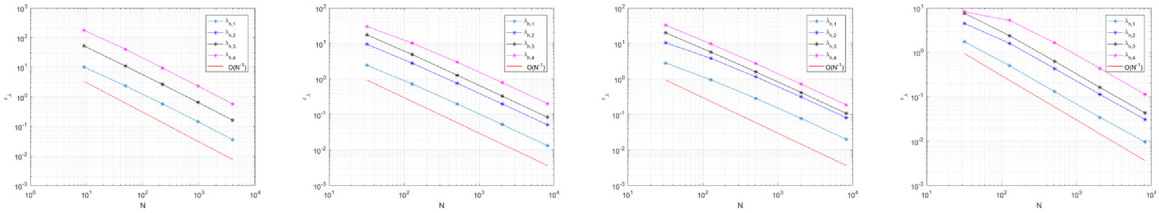

(a) $\mathcal{T}_h^1$ (b) $\mathcal{T}_h^2$ (c) $\mathcal{T}_h^3$ (d) $\mathcal{T}_h^4$

Fig. 3. Test 5.1: the error of the first four Laplace eigenvalues with $l = 1$ on Ω_S.

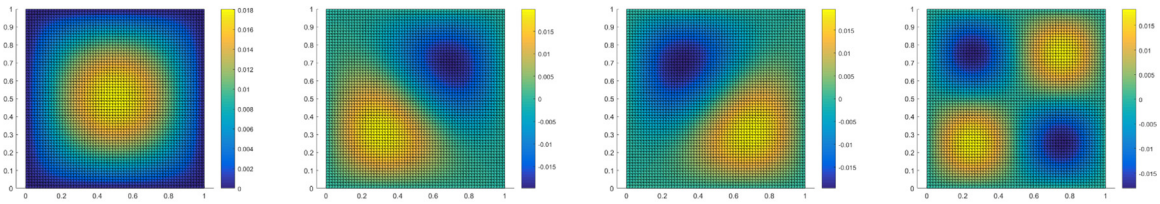

(a) $u_{h,1}$ (b) $u_{h,2}$ (c) $u_{h,3}$ (d) $u_{h,4}$

Fig. 4. Test 5.1: the eigenfunctions $u_{h,1}$, $u_{h,2}$, $u_{h,3}$, $u_{h,4}$ corresponding to the first four Laplace eigenvalues on Ω_S.

Table 3
Test 5.1: the first four Laplace eigenvalues computed by the free-stabilization VEM on Ω_L.

l	Mesh	N	$\lambda_{h,1}$	$\lambda_{h,2}$	$\lambda_{h,3}$	$\lambda_{h,4}$
0	$\mathcal{T}_h^5$	33	10.77440882052	16.62210158728	22.82025694850	35.23842730922
		161	9.96597664959	15.55728824790	20.50235202837	30.95286399930
		705	9.74081708048	15.28795492786	19.92958532961	29.87930353889
		2945	9.67295070631	15.22004762614	19.78677937819	29.61096291850
		12033	9.65120310773	15.20297050346	19.75110002634	29.54385796069
1	$\mathcal{T}_h^6$	157	9.88606427975	15.56225054523	20.35813473742	30.86614740761
		338	9.75796007115	15.37602445689	20.04017615857	30.16239849230
		712	9.70680617093	15.28533194786	19.88431307447	29.83734695203
		1481	9.67405948783	15.23943479470	19.80967980950	29.67445574870
		3204	9.65909767407	15.21789270319	19.77408325667	29.59878577210

method. These phenomena with $l = 0, 1$ are in agreement with the above theoretical claim. In addition, Fig. 4 shows the eigenfunctions related to the first four eigenvalues plotted by using the finest non-convex mesh with $l = 1$.

The second test is used to the Laplace eigenvalue problem on the L-shaped $\Omega_L = [-1, 1]^2 \setminus ((0, 1] \times [-1, 0))$, which leads that the convergence order of the eigenvalue related to the singular eigenfunction is lower than $O(N^{-1})$. Since there is not known exact solution, we compute the first four reference eigenvalues by using the linear Lagrange FEM with 48641 DoFs as follows:

$$\lambda_1 \approx 9.64125663380,\ \lambda_2 \approx 15.19761062264,\ \lambda_3 \approx 19.73995197638,\ \lambda_4 \approx 29.52288014989.$$

In Table 3, we display the numerical results of the free-stabilization VEM on uniformly refined triangular mesh $\mathcal{T}_h^5$ and Voronoi mesh $\mathcal{T}_h^6$ with $l = 0, 1$, respectively. The sample meshes are shown in the subfigures (a) and (c) of Fig. 5. We can also observe from the subfigures (b) and (d) of Fig. 5 that the convergence rates of the second, third and fourth eigenvalues are $O(N^{-1})$. However, the error of the first eigenvalue converges at the order of lower than $O(N^{-1})$. This phenomenon is because the eigenfunction corresponding to the first eigenvalue is singular at the origin of the non-convex domain, which is also in agreement with the theoretical result.

5.2. The Steklov eigenvalue problem

In the section, we consider the other Laplacian eigenvalue problem: Steklov eigenvalue problem, i.e., boundary eigenvalue problem, whose *a priori* and *a posteriori* VEMs have been analyzed in [18,19], respectively. The test of this subsection is to compute the following Steklov eigenvalue problem [18]: find $u \neq 0$ and $\lambda \in \mathbb{R}$ such that

$$\Delta u = 0 \text{ in } \Omega,\quad \nabla u \cdot \boldsymbol{\nu} = \lambda u \text{ on } \partial\Omega_0,\ \nabla u \cdot \boldsymbol{\nu} = 0 \text{ on } \partial\Omega_1,\quad \partial\Omega = \overline{\partial\Omega_0} \cup \overline{\partial\Omega_1}, |\partial\Omega_0| \neq 0,$$

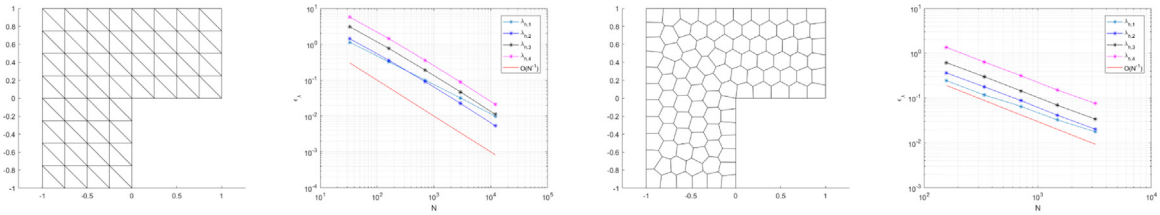

(a) $\mathcal{T}_h^5$ (b) $\mathcal{T}_h^5$ (c) $\mathcal{T}_h^6$ (d) $\mathcal{T}_h^6$

Fig. 5. Test 5.1: basic sample meshes and the error of the first four Laplace eigenvalues on Ω_L.

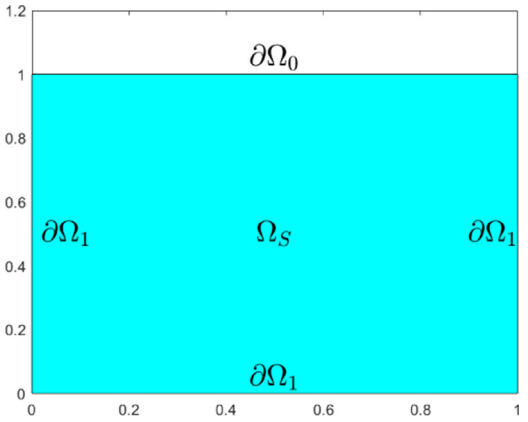

Fig. 6. Test 5.2: sloshing in the square domain Ω_S.

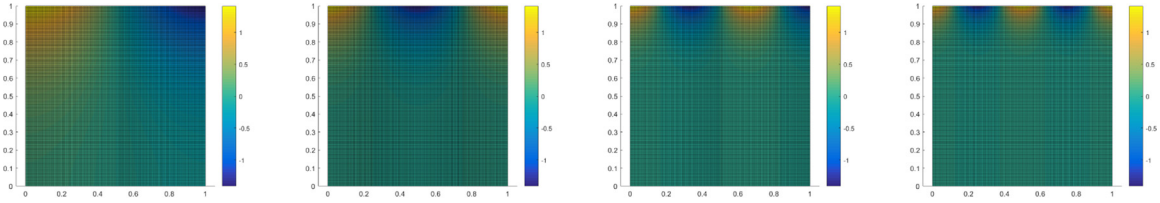

(a) $u_{h,1}$ (b) $u_{h,2}$ (c) $u_{h,3}$ (d) $u_{h,4}$

Fig. 7. Test 5.2: the eigenfunctions $u_{h,1}$, $u_{h,2}$, $u_{h,3}$, $u_{h,4}$ corresponding to the first four Steklov eigenvalues on Ω_S.

by using the free-stabilization VEM as follows: find $(\lambda_h, u_h) \in \mathbb{R} \times \mathcal{V}_{1,\ell}$ such that

$$a_h(u_h, v_h) = \lambda_h \langle u_h, v_h \rangle, \quad \forall v_h \in \mathcal{V}_{1,\ell},$$

where $\langle u_h, v_h \rangle = \int_{\partial\Omega_0} u_h v_h$ and $\mathcal{V}_{1,\ell} = \{v \in H^1(\Omega) : v|_E \in \mathcal{V}_{1,l}(E), \ \forall E \in \mathcal{T}_h\}$. Note that the term $\langle u_h, v_h \rangle$ is computable since u_h and v_h are piecewise polynomials on all boundary edges. Obviously, the above theoretical derivation can be generalized to the problem.

We consider the sloshing problem of a fluid contained in the square domain Ω_S with a horizontal free surface $\partial\Omega_0$, as shown in Fig. 6. We obtain from [18] that the exact Steklov eigenvalues and corresponding eigenfunctions for this problem are

$$\lambda_i = i\pi \tanh(i\pi), \qquad u_i(x, y) = \cos(i\pi x)\sinh(i\pi y), \quad i \in \mathbb{N}.$$

In practice, since the matrix obtained from the right-hand term $\langle u_h, v_h \rangle$ is relative sparse, which leads that the solver *eigs* in MATLAB does not work, we display in Table 4 the numerical results obtained by the uniformly refiner meshes $\mathcal{T}_h^1$, $\mathcal{T}_h^2$, $\mathcal{T}_h^3$ and $\mathcal{T}_h^4$ on Ω_S. The exact eigenvalues are also reported in the last row for comparison. It can be seen from Table 4 that the convergence rate also coincides with the theoretical result for the Steklov problem. Finally, the eigenfunctions related to the first four Steklov eigenvalues are plotted in Fig. 7.

Table 4
Test 5.2: the first four Steklov eigenvalues computed by the free-stabilization VEM with $l = 1$ on Ω_S.

Mesh	N	$\lambda_{h,1}$	$\lambda_{h,2}$	$\lambda_{h,3}$	$\lambda_{h,4}$
$\mathcal{T}_h^1$	1089	3.15203962584	6.46333770224	10.02720944963	13.97674072988
	4225	3.13543069262	6.32846359729	9.57736320578	12.92679391497
	16641	3.13126907925	6.29448957060	9.46305577765	12.65702187942
	rate	−1.02218787335	−1.01013652255	−1.00875384990	−1.00686363197
$\mathcal{T}_h^2$	640	3.24062789327	7.95777285249	11.65388495689	15.70999628035
	2304	3.16024100652	6.71487868000	9.76311408642	13.55148341603
	8704	3.13810785672	6.39877761741	9.50922134668	12.85113604956
	rate	−0.98238657623	−0.99114660445	−1.04425544075	−0.93375726452
$\mathcal{T}_h^3$	640	3.16292156148	6.73592954349	11.44083435309	14.63387091500
	2304	3.14228042768	6.39474811458	10.34578064883	12.97087925857
	8704	3.13326372785	6.31695086918	9.57782541246	12.66592366717
	rate	−0.97730825728	−0.89851006920	−1.35028645842	−1.05480738129
$\mathcal{T}_h^4$	833	3.14203957677	6.34430922429	9.38784944300	12.92792187634
	3201	3.13366858598	6.30747627833	9.49087080700	12.68431517339
	12545	3.13101366339	6.29019394789	9.44311476984	12.59456719709
	rate	−0.88382413773	−0.90677751597	−0.93870984435	−1.04770255296
Exact eigenvalues		3.12988103563	6.28314148410	9.42477783801	12.56637061405

6. Conclusion

In this paper, we have presented the *a priori* error estimates for the free-stabilization VEM of the Laplacian eigenvalue problem theoretically and numerically. The free-stabilization VEM of the eigenvalue problem has never been targeted before and is the main topic of the present work. The proposed free-stabilization VEM has the optimal convergence rate and numerical results demonstrate the optimal convergence. Next, we will consider the *a posteriori* error estimates for the free-stabilization VEM. The free-stabilization VEM can also be applied to non-self-adjoint elliptic eigenvalue problems, which are under our investigation currently.

Acknowledgments

We wish to thank the referee for his/her constructive comments and suggestions. The work is supported by the China Scholarship Council (No. 202106280167), Fundamental Research Funds for the Central Universities, China (No. xzy022019040) and National Natural Science Foundation of China (No. 12171385).

References

[1] A. Bermúdez, R. Durán, A. Muschietti, R. Rodríguez, J. Solomin, Finite element vibration analysis of fluid-solid systems without spurious modes, SIAM J. Numer. Anal. 32 (1995) 1280–1295.
[2] F. Cakoni, D. Colton, S. Meng, P. Monk, Stekloff eigenvalues in inverse scattering, SIAM J. Math. Anal. 76 (4) (2016) 1737–1763.
[3] R. Rannacher, Nonconforming finite element methods for eigenvalue problems in linear plate theory, Numer. Anal. 33 (1979) 23–42.
[4] Y. Saad, J. Chelikowsky, S. Shontz, Numerical methods for electronic structure calculations of materials, SIAM Rev. 52 (1) (2010) 3–54.
[5] P. Antonietti, A. Buffa, I. Perugia, Discontinuous Galerkin approximation of the Laplace eigenproblem, Comput. Methods Appl. Mech. Engrg. 195 (2006) 3483–3503.
[6] V. Calo, M. Cicuttin, Q. Deng, A. Ern, Spectral approximation of elliptic operators by the hybrid high-order method, Math. Comp. 88 (2019) 1559–1586.
[7] J. Kuttler, Direct methods for computing eigenvalues of the finite difference Laplacian, SIAM J. Numer. Anal. 11 (1974) 732–740.
[8] Q. Zhai, H. Xie, R. Zhang, Z. Zhang, Acceleration of weak Galerkin methods for the Laplacian eigenvalue problem, J. Sci. Comput. 79 (2019) 914–934.
[9] I. Babuška, J. Osborn, Finite element Galerkin approximation of the eigenvalues and eigenfunctions of selfadjoint problems, Math. Comp. 52 (186) (1989) 275–297.
[10] I. Babuška, J. Osborn, Eigenvalue problems, in: Handbook of Numerical Analysis, Vol. II, North-Holland, Amsterdam, 1991, pp. 641–787.
[11] D. Boffi, Finite element approximation of eigenvalue problems, Acta Numer. 19 (2010) 1–120.
[12] B. Mercier, J. Osborn, J. Rappaz, P.A. Raviart, Eigenvalue approximation by mixed and hybrid methods, Math. Comp. 36 (1981) 427–453.
[13] J. Sun, A. Zhou, Finite Element Methods for Eigenvalue Problems, CRC Press, 2016.
[14] L. Beirão Da Veiga, F. Brezzi, A. Cangiani, G. Manzini, L.D. Marini, A. Russo, Basic principles of virtual element methods, Math. Models Methods Appl. Sci. 23 (1) (2013) 199–214.
[15] F. Brezzi, The great beauty of VEMs, in: Proceedings of the International Congress of Mathematicians, Seoul, ICM, vol. 1, 2014, pp. 217–235.
[16] F. Brezzi, L.D. Marini, Finite elements and virtual elements on classical meshes, Vietnam J. Math. (2021) http://dx.doi.org/10.1007/S10013-021-00474-Y.
[17] G. Monzón, A virtual element method for a biharmonic steklov eigenvalue problem, Adv. Pure Appl. Math. 10 (4) (2019) 325–337.
[18] D. Mora, G. Rivera, R. Rodríguez, A virtual element menthod for the steklov eigenvalue problem, Math. Models Methods Appl. Sci. 25 (8) (2015) 1421–1445.

[19] D. Mora, G. Rivera, R. Rodríguez, A posteriori error estimates for a virtual element menthod for the steklov eigenvalue problem, Comput. Math. Appl. 74 (9) (2017) 2172–2190.
[20] F. Gardini, G. Manzini, G. Vacca, The nonconforming virtual element method for eigenvalue problems, ESAIM Math. Model. Numer. Anal. 53 (3) (2019) 749–774.
[21] F. Gardini, G. Vacca, Virtual element method for second order elliptic eigenvalue problems, IMA J. Numer. Anal. 38 (4) (2017) 2026–2054.
[22] J. Meng, Y. Zhang, L. Mei, A virtual element method for the Laplacian eigenvalue problem in mixed form, Appl. Numer. Math. 156 (2020) 1–13.
[23] O. Čertík, F. Gardini, G. Manzini, L. Mascotto, G. Vacca, The virtual element method for eigenvalue problems with potential terms on polytopic meshes, Appl. Math. 63 (2018) 333–365.
[24] O. Čertík, F. Gardini, G. Manzini, L. Mascotto, G. Vacca, The *p*- and *hp*-versions of the virtual element method for elliptic eigenvalue problems, Comput. Math. Appl. 79 (7) (2020) 2035–2056.
[25] L. Beirão Da Veiga, D. Mora, G. Rivera, R. Rodríguez, A virtual element method for the acoustic vibration problem, Numer. Math. 136 (3) (2017) 725–763.
[26] J. Meng, L. Mei, A mixed virtual element method for the vibration problem of clamped Kirchhoff plate, Adv. Comput. Math. 46 (2020) 68.
[27] D. Mora, G. Rivera, I. Velásquez, A virtual element method for the vibration problem of kirchhoff plates, ESAIM Math. Model. Numer. Anal. 52 (4) (2018) 1437–1456.
[28] D. Mora, I. Velásquez, Virtual element for the buckling problem of Kirchhoff-Love plates, Comput. Methods Appl. Mech. Engrg. 360 (1) (2020) 112687.
[29] D. Mora, G. Rivera, A priori and a posteriori error estimates for a virtual element spectral analysis for the elasticity equations, IMA J. Numer. Anal. 40 (2020) 322–357.
[30] J. Meng, G. Wang, L. Mei, A lowest-order virtual element method for the Helmholtz transmission eigenvalue problem, Calcolo 58 (2021) 2.
[31] D. Mora, I. Velásquez, A virtual element method for the transmission eigenvalue problem, Math. Models Methods Appl. Sci. 28 (14) (2018) 2803–2831.
[32] F. Lepe, G. Rivera, A virtual element approximation for the pseudostress formulation of the Stokes eigenvalue problem, Comput. Methods Appl. Mech. Engrg. 379 (2021) 113753.
[33] D. Boffi, F. Gardini, L. Gastaldi, Virtual element approximation of eigenvalue problems, 2020, arXiv:2012.15660v1.
[34] D. Boffi, F. Gardini, L. Gastaldi, Approximation of PDE eigenvalue problems involving parameter dependent matrices, Calcolo 57 (2020) 41.
[35] S. Berrone, A. Borio, F. Marcon, Lowest order stabilization free virtual element method for the Poisson equation, 2021, arXiv:2103.16896v1.
[36] B. Ahmad, A. Alsaedi, F. Brezzi, L.D. Marini, A. Russo, Equivalent projections for virtual element methods, Comput. Math. Appl. 66 (3) (2013) 376–391.
[37] S.C. Brenner, R.L. Scott, The mathematical theory of finite element methods, in: Texts Appl. Math., Vol. 15, Springer-Verlag, New York, 2008.
[38] A. Gangiani, E.H. Georgoulis, T. Pryer, O.J. Sutton, A posteriori error estimates for the virtual element method, Numer. Math. 137 (4) (2017) 857–893.